IEEE Access
Multidisciplinary | Rapid Review | Open Access Journal

Received June 5, 2021, accepted June 17, 2021, date of publication June 21, 2021, date of current version June 29, 2021.

Digital Object Identifier 10.1109/ACCESS.2021.3091309

A Unified Method for Deinterleaving and PRI Modulation Recognition of Radar Pulses Based on Deep Neural Networks

JIN-WOO HAN[1,2] **AND CHEONG HEE PARK**[1]

[1]Department of Computer Science and Engineering, Chungnam National University, Daejeon 34134, South Korea
[2]Defense Science and Technology Academy, Agency for Defense Development, Daejeon 34186, South Korea

Corresponding author: Cheong Hee Park (cheonghee@cnu.ac.kr)

ABSTRACT In the modern electronic warfare signal environment, multiple radar signals of high density are mixed and received, and separating them into signals for each emitter is an essential step for emitter identification. Each radar has its own pulse repetition interval (PRI), which is a key parameter for deinterleaving pulse trains. The PRI is modulated in various forms depending on the purpose of the radar operation, and analyzing the mean PRI and the modulation type of PRI is the core of electronic warfare signal processing. Many existing papers have tried separate independent approaches for deinterleaving and for PRI modulation recognition. However, many distortions are unintentionally generated in the process of extracting the pulse train using the PRI estimated through deinterleaving for the PRI modulation recognition. This degrades the modulation recognition performance. In this paper, we propose a unified method for the deinterleaving and PRI modulation recognition of radar pulses using deep learning-based multitasking learning. The simulation results demonstrate the good performance of the proposed method for deinterleaving and modulation recognition, compared to the conventional method, and prove that the proposed method is robust in noisy radar signal environments.

INDEX TERMS Multi-task learning(MTL), deep learning, PRI, deinterleaving, modulation, electronic warfare.

I. INTRODUCTION

Electronic warfare support(ES) improves the survivability of allies by providing early warning, through the process of analyzing received emitter signals and identifying the emitters by comparing them with identification libraries. However, in operation, electronic warfare systems designed for emitter alerts and the self-defense of ships and aircraft face a complex signal environment, in which multiple emitter signals are mixed and signal distortions such as missing and spurious pulses are included [1].

In order to identify an emitter with high accuracy in such a signal environment, it is essential to deinterleave the pulse train of each emitter signal and recognize the modulation type of each pulse train. The purpose of deinterleaving the pulse train is to separate the corresponding pulse train for each emitter signal from the received pulse signal. In a signal environment with low signal density and low distortion, it is possible to deinterleave the received pulse signals using only signal measurement variables such as frequency, direction of arrival, and pulse width. However, in the modern electronic warfare signal environment, emitter signals with various changing signal characteristics can arrive from a similar direction at the same time, and the density of the emitter signals has been gradually increasing. As a result, the deinterleaving of pulse trains has become an increasingly challenging task [1]. In addition, artificial signal distortion, such as the jamming pulse in [2], is also being employed for anti-electronic warfare.

To deinterleave a pulse train, the pulse repetition interval (PRI) information, which is derived from the time of arrival (TOA) of each pulse, is used. PRI is a key characteristic of radar emitters and refers to the repetition period of the pulses transmitted by the radar. Given the TOA sequence of the radar signal, the PRI sequence is defined as:

$$p(i) = t_{i+1} - t_i, \quad i = 0, 1, \ldots, N-1 \tag{1}$$

The associate editor coordinating the review of this manuscript and approving it for publication was Hasan S. Mir.

where t_i is the TOA of the i-th pulse and N is the total number of received pulses. Radars search or track targets by sending and receiving pulses, using their own unique PRI characteristics. Therefore, in electronic warfare support, it is necessary to deinterleave the pulse trains of each emitter signal from the received pulse signal by estimating the PRI based on the continuity and regularity of the received pulse.

Fig. 1(a) shows the general signal processing flow in ES. The deinterleaving of pulse trains is performed using Pulse Description words(PDWs) collected from the receiver, and then pulse trains are extracted using PRI information obtained through deinterleaving. Deinterleaving is again performed on the remaining pulses. This process continues until the number of remaining pulses falls below the threshold. PRI modulation recognition is performed for each extracted pulse train. When the modulation recognition is completed, the PRI information and modulation recognition result are compared with the built-in library to identify the emitter.

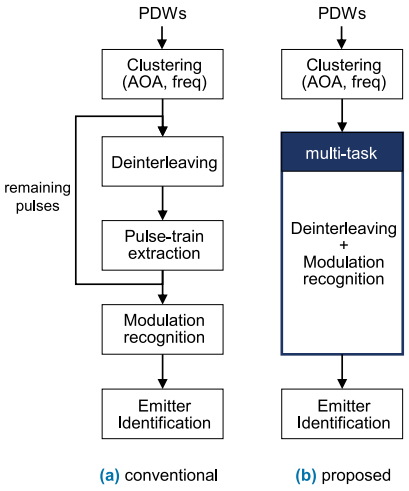

FIGURE 1. Signal processing flow in ES.

Since the result of deinterleaving is used as an input to the PRI modulation recognition step, the performance of the deinterleaving greatly affects the performance of the PRI modulation recognition. If deinterleaving and PRI modulation recognition are performed independently, the performance of emitter identification may be degraded, even in a good signal environment where signal distortions such as missing pulses do not exist. For a pulse train with modulation where the PRI type is not stable, pulse distortion can occur in the pulse train extraction step after deinterleaving. It may act as a burden on the PRI modulation recognition step and degrade the overall performance.

To overcome the limitation of separated processes and ensure highly accurate emitter analysis, it is essential to perform deinterleaving and PRI modulation recognition at the same time. Fig. 1(b) illustrates the proposed method, which combines deinterleaving and modulation recognition. We train a convolutional neural network(CNN) which performs deinterleaving and PRI modulation recognition at the same time under the Multi-Task Learning (MTL) framework. The proposed unified method is designed to take advantage of the interrelationship between the two tasks to improve learning efficiency, and the accuracy of deinterleaving and PRI modulation recognition. As far as we know, this is a new approach in the field of electronic warfare signal processing.

The rest of the paper is organized as follows. Section II describes the conventional deinterleaving and PRI modulation recognition methods. In Section III, the concept of PRI modulation and distortion is introduced, and in Section IV, a unified method of deinterleaving and PRI modulation type recognition based on MTL using deep neural networks is proposed. Section V presents the simulation results under various conditions. Section VI shows the effect of the parameter values on the proposed model, and we conclude in Section VII.

II. RELATED WORKS

Research fields of electronic warfare signal processing include intra-pulse modulation recognition, deinterleaving, PRI modulation recognition, and emitter identification. Intra-pulse modulation recognition is a task to classify modulation of frequency or phase within the pulse. Deep learning methods such as CNN and LSTM have been actively applied for intra-pulse modulation [3]–[5] and the construction of a separate non-negative matrix factorization network was proposed in [6]. Emitter identification is a task to identify emitters through comparison with a built-in library using parameters extracted through signal analysis. [7] proposed a method to improve the performance of classifiers for emitter identification even in situations where there are many missing data. Deinterleaving and PRI modulation recognition have been one of the main research topics in ES. However, in most research they have been studied separately and independently.

A. DEINTERLEAVING

The field of deinterleaving started with histogram-based approaches such as cumulative difference histrogram (CDIF) [8] and sequential difference histogram (SDIF) [9]. The histogram is generated for the TOA of each pulse, and the PRI is estimated by comparing it with a predefined threshold. In the histogram method, the amount of calculation increases rapidly with the number of pulses, and the performance difference becomes larger with the size of the histogram bin. Also, there is ambiguity when setting the threshold, so it exhibits low performance for pulse trains with non-stable PRI. Other studies have been conducted to address the speed problem of the histogram method and the PRI estimation problem [10], [11], but the ambiguity of the histogram bin still exists.

In [12], a PRI estimation method based on Discrete Fourier Transform (DFT) was proposed, but it had low estimation performance in a noisy environment. The concept of phase and estimated PRI based on Continuous Wavelet Transform (CWT) was introduced in [13]. Although the method

showed relatively robust performance against noise, similar to other existing methods, it had the ambiguity of threshold setting. However, the CWT method had the potential of confirming changes in PRI over time.

[14] proposed a method called PRI transform. Similar to the CWT method, the PRI transform estimated mean PRI using the phase information between pulses, and showed robust performance against noise, but performance degraded depending on the detection range of PRI and the rate of variation in the non-stable PRI signal. Various studies have been conducted to resolve the shortcomings of the PRI transform. Studies were conducted to solve the problem of performance degradation due to the upper limit of PRI and stagger PRI estimation problem [15], and to improve the speed by changing the phase calculation to linear addition [16]. In addition, to improve performance for jittered PRI and stagger PRI, a procedural method using two versions of PRI transform [17] and a method of merging the extracted EDW (Emitter Description Word) [18] have been proposed. [19] proposed a method of calculating the PRI transform for each window by covering the PRI transform with a short time window like CWT, and estimating the PRI through a total of 64 snapshots. However, only the contents of the snapshot configuration were reported, and no information was presented on how to estimate the PRI. In addition, another study proposed a method of processing a large jitter rate signal through gradient analysis of the input signal [20]. A method of extracting features by converting the collected signal into a 2D image and estimating the PRI using a rough transform [21] was also proposed.

Recently, methods using deep learning have also been proposed. In [22], a method of estimating PRI using pulse width and PRI as inputs of the recurrent neural network was proposed, but this must be repeated continuously through re-input after extracting the pulse train. It did not take into account the possible ambiguities in the pulse width. In [23], a denoising autoencoder was used to perform deinterleaving, and for the first time, the pulse trains were automatically deinterleaved by the output of the autoencoder without artificially extracting the pulse train. However, this method, which focuses on removing noise, has a disadvantage, in that it is not possible to extract a jittered PRI pulse train composed of a certain range of noise. [24] proposed a method of estimating PRI using the CWT result of the input pulse trains as an input to the MLP network. In [25], a method of tracking pulse amplitude to improve the performance of deinterleaving was proposed.

In most of the studies mentioned so far, performance deteriorates rapidly in environments with various signal distortions. In addition, since only methods of estimating PRI are considered, the pulse trains of each emitter must be extracted to recognize the PRI modulation, and distortion is not considered at all. Since the focus is only on deinterleaving rather than improving the overall accuracy of electronic warfare signal processing, they are limited when it comes to achieving the final goal of accurately identifying emitters.

B. PRI MODULATION RECOGNITION

There are two types of PRI modulation recognition, conventional feature-based methods and recent deep learning-based methods. [26] proposed a method to calculate the autocorrelation function (ACF) using TOA to recognize the PRI modulation type by comparing it with a predefined threshold. Another ACF-based study was also proposed for the subtype recognition of complex PRI [27], such as saturated sinusoidal modulation. [28] proposed a machine learning-based PRI estimation method. He defined the signum function for the input TOA, extracted 62 features, and estimated the PRI modulation using Multi Layer Perceptron (MLP), but there were several limitations, including the number of input signals. A method [29] was proposed which utilized features such as continuity and linearity, and used the signum function in [28]. Another method [30] of utilizing features such as stationary and symmetry was also proposed. The authors in [31] used features such as modified Shannon's entropy and kurtosis after symbolizing TOA sequences, and in [32], features such as normalized jump energy and SP-curve for PRI modulation recognition were used. In addition, a study on various emitter scenarios was also presented that used a wavelet transform and histogram in combination through various procedures [33]. [34] proposed a PRI modulation recognition method through wavelet-based feature extraction. In [35], a hierarchical classification method using histogram-based features and sequential information-based features was proposed.

Recently, modulation recognition methods using deep learning have also been proposed. In [36], a method of recognizing PRI modulation using a CNN without performing a preprocessing process on the input signal was proposed. After obtaining ACF results for the input signal, a method of defining an ACSE network using the features extracted from the ACF result as an input, was also proposed [37]. [38] proposed a PRI modulation type recognition method using attention-based RNN, which worked well on time series data.

III. PRI MODULATION AND DISTORTION

PRI modulation types include stable (STB), stagger (STG), dwell & switch (D&S), jittered (JTR) and pattern, while pattern includes wobulated (WOB), sliding(+) (SLP) and sliding(−) (SLM). The stable PRI type always has the same PRI value over time, but in non-stable PRI modulation types, PRI values change over time, as shown in Fig. 2. The stagger signal is a combination of several signals with the same period, and the dwell & switch signal dwells in one PRI and then switches to another PRI under certain conditions. For jittered, wobulated, sliding(+), sliding(−) signals, the PRI value changes pulse by pulse, and these types change the PRI value in a specific form or randomly.

Pulse distortions can occur due to the complex signal environment itself, deinterleaving of electronic warfare equipment, or poor pulse train extraction performance. Pulse distortions eventually degrade the estimation performance of

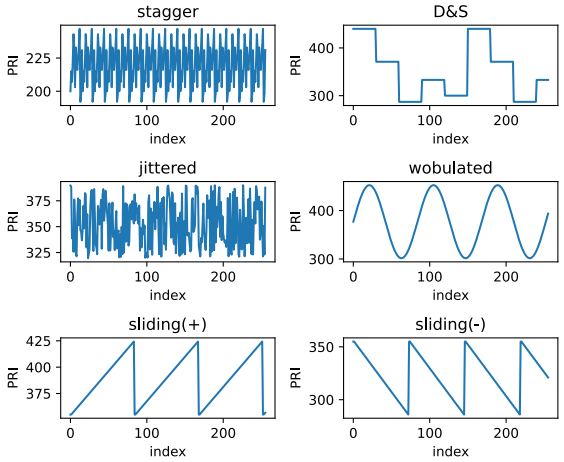

FIGURE 2. PRI modulations for non-stable PRI.

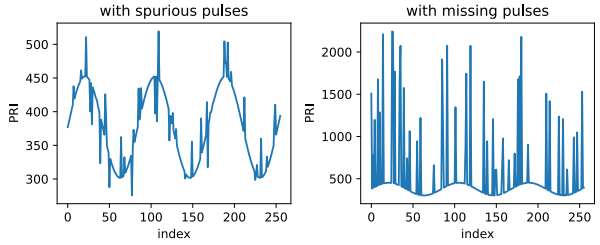

FIGURE 3. Distortions in a wobulated signal by the signal environment.

the parameter used to identify the emitter. The spurious pulse and missing pulse in Fig. 3 are representative pulse distortion results that occur in the signal environment. However, unlike distortions caused by such a signal environment, a distortion that is generated during the process of estimating the emitter's PRI information and extracting the corresponding pulse train can greatly influence both the extracted pulse train and the remaining pulses.

Fig. 4 illustrates the simulation results when extracting only the wobulated signal from the pulse train using a conventional deinterleaving process, in which a wobulated signal and a jittered signal having the same mean PRI are mixed. The extraction was performed under the assumption that there are no spurious pulses or missing pulses. Distortions by deinterleaving are particularly severe when multiple emitters with similar mean PRI are present at the same time. This distortion occurs because there is no PRI modulation information in the process of selecting the next pulse to be extracted after one pulse is extracted.

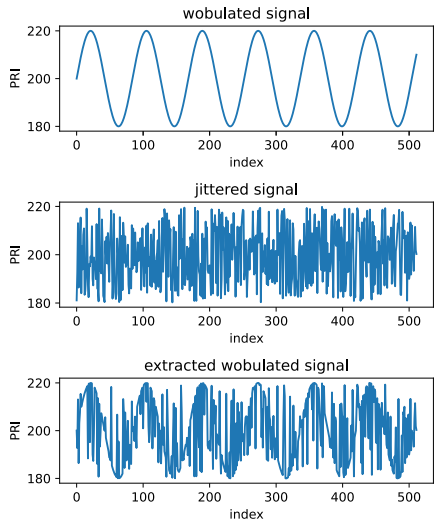

FIGURE 4. Distortions by the deinterleaving performance.

In the pulse train extraction step, since there is no accurate information about the modulation type of the PRI, it must be extracted using only the mean PRI information. Hence, all pulses within a specific range around the mean PRI can be candidates for extraction. Fig. 4 clearly shows that the pulse distortions arising from traditional deinterleaving and pulse train extraction methods should not be overlooked.

IV. PROPOSED METHOD

To overcome the shortcomings of conventional electronic warfare signal processing, we propose a unified deinterleaving and PRI modulation recognition method based on multi-task learning with a CNN. To apply supervised learning-based deep learning, the input data and labels for ground truth must be defined. CWT is a signal processing tool for time-frequency analysis of signals that provides high-accuracy time and frequency localization. CWT can be simplified as a function of cosine and sine by using Euler's formula, so it is easy to apply to real-time embedded systems such as electronic warfare systems. In addition, it is possible to check the frequency change over time by applying CWT for the sliding windows on the pulse trains. Therefore, we use CWT to construct inputs of our proposed deep neural network, considering the advantages of easy implementation and 2D image generation representing deinterleaving and PRI modulation analysis at once. CWT results [13] are visually similar to images and can be used to confirm changes in PRI over time. The label for the target is composed of a two-dimensional array containing the PRI and modulation information, and label propagation is proposed to compensate for the deinterleaving error. The proposed CNN-based MTL model combines three loss functions, defined for mean PRI estimation and modulation type prediction, and improves performance by adding residual blocks and global average pooling. Post-processing that merges adjacent estimated PRIs is also introduced to reduce false alarms in the testing process. The overall training and testing procedure of the proposed method is shown in Fig. 5.

A. INPUT DATA CONFIGURATION

Suppose the TOA's of the received pulse train, $t_1, t_2, t_3, \ldots$, are represented as a superposition of impulses, as in [13]:

$$s(t) = \sum_j \delta(t - t_j) \tag{2}$$

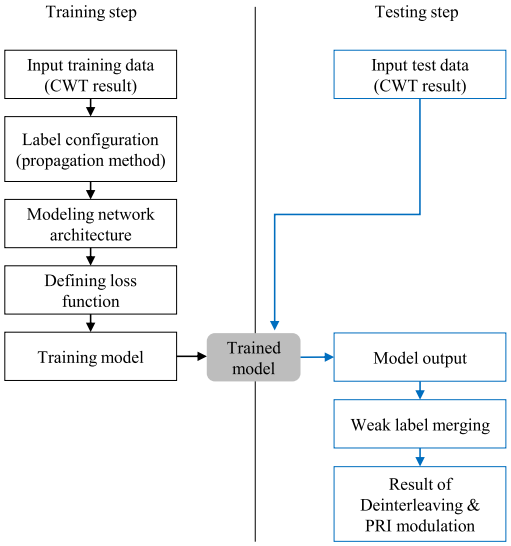

FIGURE 5. Training and testing procedure of the proposed method.

To apply wavelet transform, we define the mother wavelet as follows [13]:

$$\psi(t) = M^{-\frac{1}{2}} \chi\left(\frac{t}{M}\right) e^{2\pi it} \tag{3}$$

where $\chi(t)$ is a rectangular window of unit length defined on [-1/2, 1/2] and M denotes the size of the moving window on a pulse train which is set as the minimum number of pulses for the analysis of the mean PRI and modulation type. CWT is performed for the pulses within each window which moves forward.

The wavelet transform for $s(t)$ [13] is as follows:

$$D(T, t) = \frac{T}{M} \left| \int \psi^* \left(\frac{t' - t_w}{T}\right) s(t') dt' \right|^2 \tag{4}$$

where T is a variable for estimating mean PRI values, which are assumed to be ranged in [0,512], and t_w represents the starting time of the current window t. If the mean PRI of an emitter is S, due to the exponential function in Eq (3), $D(T, t)$ has a large value when T is the multiple of S.

The result of applying CWT to the input pulse train is three dimensional data of [window number t, T, Power]. Power is $D(T, t)$, which is the result of applying CWT at window number t. Assuming the input pulse trains are composed of stable and wobulated types of mean PRIs of 164μs and 245μs respectively. Fig. 6 compares the values of $D(T, t)$ in a single window when three different window sizes, 16, 32, and 64, are used. For high-accuracy deinterleaving, the peak value corresponding to the mean PRI of the input pulse train should be high and the peak shape needs to be sharp. A high peak value indicates that there is a high probability of a pulse train having a corresponding mean PRI, and a sharp shape indicates a high resolution PRI estimation. In the case of $M = 16$ in Fig. 6, a peak that appears to correspond to a stable PRI and a peak group that appears to be wobulated PRI are shown. However, the width of the peak corresponding to the stable PRI is large, which degrades the resolution of the PRI estimation. In addition, the peak at 82μs, which is a sub-harmonic (half PRI) of this stable PRI, is quite large. This raises concerns that can be estimated as a result of deinterleaving to the sub-harmonic. As M increases, the peak corresponding to PRI 164μs becomes sharper. This increases the resolution of the deinterleaving and the accuracy of the PRI estimation.

By applying CWT for the pulses within a moving window on the input pulse train, we obtained the image shown in Fig 7, where the values of $D(T, t)$ for each window are plotted in each column. The images in Fig. 7 were used as input in the proposed convolutional neural network. However, the sizes of the input images for CNN need to be fixed regardless of the size of a window. In order to have the same number of windows even when a different window size is used, we moved a window forward, allowing an appropriate overlap size of windows. In the case of $M = 16$ of Fig. 7, the shapes of the two modulation types, stable and wobulated, appear strongly in bright colors. As M increases, the number of pulses within a window increases and it becomes difficult to accurately represent the PRI change per pulse. M determines the set of pulses to which the wavelet transform is applied, and accordingly has a great influence on the resolution of deinterleaving and the performance of PRI modulation. It can

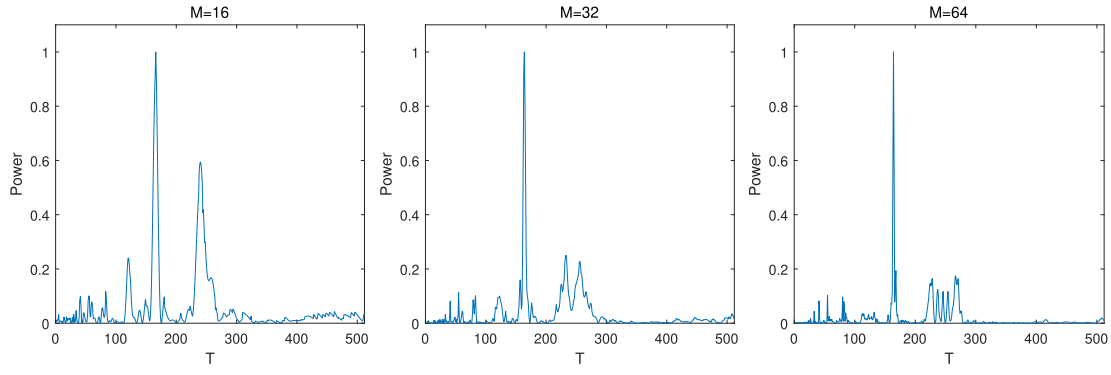

FIGURE 6. PRI estimation result according to window size M.

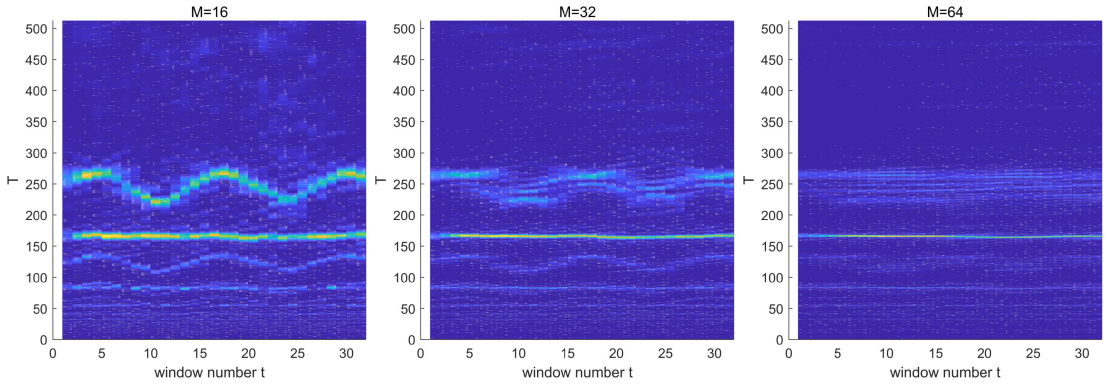

FIGURE 7. PRI changes with window size M over time.

be seen that deinterleaving and PRI modulation recognition performance are in a trade-off relationship according to M. In order to extract the mean PRI of each emitter in a situation where the pulses from multiple emitters are mixed, it is advantageous that the number of pulses to be analyzed at one time is large enough. On the other hand, the number of pulses to be analyzed at one time should be small to properly recognize the change in PRI when the PRIs are extracted by moving the window over time. Therefore, rather than using a single M value, it is necessary to properly combine the results from multiple M values, which could be advantageous for deinterleaving and PRI modulation recognition. Fig. 8 shows the results from the normalized weighted sum of the CWT results for $M = 16$ and $M = 64$ with weights 1/4 and 3/4. It clearly shows both the mean PRI and PRI modulation type. In the simulations in Section V, 32×512 sized images were constructed by using two window sizes, of $M = 16$ and $M = 64$, as the input for CNN. We also give the test results from the combination of different window sizes such as 32 and 64 or 16 and 32 in Section VI-D. In the image size of 32×512, 32 is the number of moving windows (t in Equation 4), and 512 is the range of the PRI to be detected. Hence, it is possible to change the size of the input image of a deep neural network by changing the PRI range to be detected or by changing the number of moving windows.

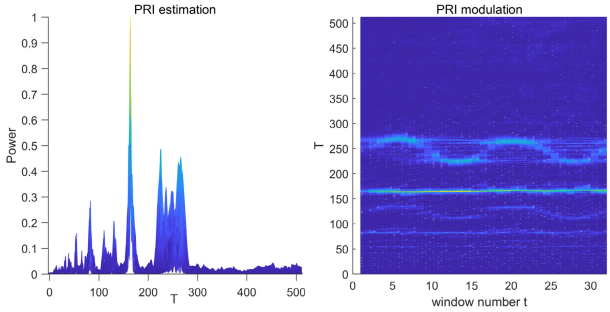

FIGURE 8. Proposed input data.

B. LABEL CONFIGURATION

In order to train a CNN model, the target label for an input data must be clearly defined. The label for our MTL model with deep neural networks must include the ground truth of both deinterleaving and PRI modulation recognition. We define a target label as a two-dimensional array where the first row contains the information for the mean PRIs and the remaining rows indicate modulation type. The value 1 in the first row means that a pulse train with a mean PRI corresponding to that index is present in the input signal. The PRI modulation type corresponding to each PRI index is encoded as a 5-digit binary vector in the column from the second row to the sixth row. Fig. 9 shows an example of the label configuration for a signal with a PRI of 205μs and a modulation wobulated type. In our simulation in Section V, the PRI range to be considered was set from 100μs to 300μs. Therefore, the target label was configured as a two-dimensional array whose column size was 201 and a row size was 6. The dwell & switch modulation type has stable PRI values within a specific range, and the stagger type always has a constant frame period, so those two types are usually analyzed first as stable type. Dwell & switch and stagger types are further recognized during post-processing. Accordingly, the dwell & switch and stagger PRI types were excluded in the experiments for PRI modulation recognition.

The peak of the CWT result for input signal may appear in some indices around the mean PRI due to pulse distortion as shown in Fig. 10. In order to reflect this observation about

	index	…	101	102	103	104	105	106	107	108	109	…
PRI flag		0	0	0	0	0	1	0	0	0	0	0
Modulation flag	STB	0	0	0	0	0	0	0	0	0	0	0
	JTR	0	0	0	0	0	0	0	0	0	0	0
	SLP	0	0	0	0	0	0	0	0	0	0	0
	SLM	0	0	0	0	0	0	0	0	0	0	0
	WOB	0	0	0	0	0	1	0	0	0	0	0

FIGURE 9. An example of label configuration as a two dimensional array.

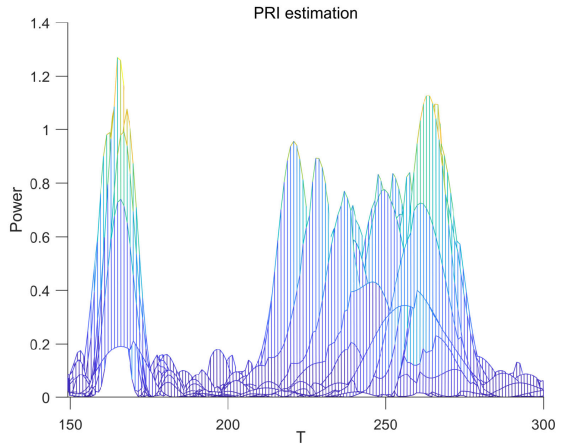

FIGURE 10. Several PRI peaks for stable and wobulated PRI.

	index	…	63	64	65	…	142	143	144	145	146	147	148	…
PRI flag		0	0.9	1	0.9	…	0.8	0.8	0.8	1	0.8	0.8	0.8	0
Modulation flag	STB	0	1	1	1	0	0	0	0	0	0	0	0	0
	JTR	0	0	0	0	0	0	0	0	0	0	0	0	0
	SLP	0	0	0	0	0	0	0	0	0	0	0	0	0
	SLM	0	0	0	0	0	0	0	0	0	0	0	0	0
	WOB	0	0	0	0	0	1	1	1	1	1	1	1	0

FIGURE 11. Label configuration after label propagation (PRI = 164μs, 245μs).

label configuration, we propose a method, called a label propagation method, that propagates the PRI and modulation flag using a margin which is set differently depending on the PRI modulation type. We set a margin of 1μs for the stable PRI type and 3μs for the non-stable PRI type. The PRI flag 1 is propagated as it is within the margin range, while the propagated value is set to a value other than 1 with a slight penalty. We set the propagated value as 0.9 for stable type and as 0.8 for non-stable types as shown in Fig. 11. As for the modulation flag, the value 1 is propagated as it is within the range in which the PRI flag is propagated.

C. NETWORK ARCHITECTURE

We propose an MTL architecture using CNN as a unified model for deinterleaving and PRI modulation recognition. CNN is a specialized kind of neural network for processing data that has a known, grid-like topology [39]. Convolutional networks have been tremendously successful in practical applications such as object detection in computer vision, and has since been widely used in various fields such as speech recognition. The proposed network model is shown in Fig. 12.

As an input the proposed network receives images with a size [1 × 32 × 512] set by the CWT process and extracts features while passing through the convolution layers. The filter used in most convolution layers of the network is a 3 × 3 size filter. In the last convolutional layer, a 1 × 1 size filter is used to adjust the size of the output channel to 1206, which is 201(PRI)×6(modulation). After features are compressed through convolution and maxpooling, representative features for each channel are extracted through global average pooling (GAP) [40]. In conventional CNN, after a feature is extracted through CNN, classification is performed through a number of fully connected layers, which is likely to cause overfitting. Instead of adding several fully connected layers on top of the feature maps, global average pooling takes the average of each feature map, and the resulting vector is fed directly into the last dense layer. In order to prevent gradient loss as the depth of the network increases, we composed some convolutional layers in the network as a residual block. The residual block adds the identity to the convolution result and leaky-relu activation as a shortcut connection [41]. Table 1 details the output shape and number of parameters for each layer of the proposed model.

TABLE 1. Number of parameters in the proposed network.

Layer	Output shape	#Parameters
Input	1 × 32 × 512	-
layer1 (convolution)	16 × 32 × 512	208
layer2 (residualblock+maxpooling)	32 × 16 × 256	14,080
layer3 (residualblock+maxpooling)	64 × 8 × 128	55,808
layer4 (residualblock+maxpooling)	128 × 4 × 64	222,208
layer5 (residualblock+maxpooling)	256 × 2 × 32	886,784
layer6 (residualblock+maxpooling)	512 × 1 × 16	3,543,040
layer7 (convolution)	1024 × 1 × 16	4,722,688
layer8 (convolution)	1024 × 1 × 16	9,441,280
layer9 (convolution)	1024 × 1 × 16	1,236,150
layer10 (GAP)	1206	-
layer11 (dense)	1206	1,455,642
layer12 (reshape)	201 × 6	-
total parameters		21,577,888
trainable parameters		21,569,792

D. LOSS FUNCTION

MTL is a deep learning method that derives results by sharing the characteristics of an input for two or more tasks [42]. We used hard parameter sharing to share most of the network parameters for MTL. The proposed method was performed using three loss functions for the last output at the top of the network. We set up the tasks for the deinterleaving task and the PRI modulation recognition task. It is important that the deinterleaving task accurately finds the mean PRI of the active emitter, but it is also important not to generate false alarms. Therefore, we divided the deinterleaving task into an emitter estimation task and a non-emitter suppression task. As described in Section IV-B, the output of the proposed network is a two-dimensional array, where the first row is the PRI flag, and each column in the remaining subarray represents 5-digits, encoding for the PRI modulation type. For the input image X, the two-dimensional array representing the ground truth label, designated as Y, is configured by the label propagation method explained in Section IV-B. We denote the output of the network as $\hat{Y}$. $Y_{i,j}$ and $\hat{Y}_{i,j}$ are the i,j-th element of Y and $\hat{Y}$.

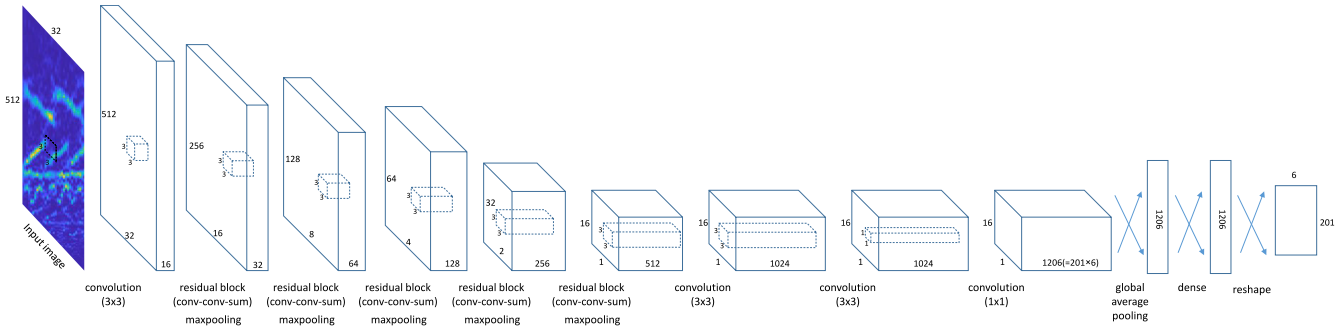

FIGURE 12. Proposed network model.

The goal of the emitter estimation task is to estimate the emitter PRI accurately, which is a true positive prediction for the input PRI. We define the loss function for the emitter estimation task as follows:

$$\mathcal{L}_T = \sum_i Y_{1,i}(Y_{1,i} - \hat{Y}_{1,i})^2 \tag{5}$$

where $Y_{1,i}$ is the ground truth for emitter PRI. The loss function measures the difference between the true PRI values and predicted PRI values in PRI indices where the emitter PRI exists.

The non-emitter suppression task aims to suppress a non-emitter PRI flag from being 1. In other words, its goal is to prevent a false positive prediction for PRI. The loss function for the non-emitter suppression task is as follows:

$$\mathcal{L}_F = \sum_i (1 - Y_{1,i})(Y_{1,i} - \hat{Y}_{1,i})^2 \tag{6}$$

The loss function has been designed to measure the difference between the true PRI values and predicted PRI values in PRI indices where an emitter PRI does not exist. In electronic warfare, this is also called a false alarm.

The PRI modulation recognition task processes the prediction of PRI modulation type for each emitter PRI. The loss function for the PRI modulation recognition task is defined as follows:

$$\mathcal{L}_M = \sum_i Y_{1,i}(Y_{2:6,i} - \hat{Y}_{2:6,i})^2 \tag{7}$$

where $Y_{2:6,i}$ denotes the i-th column in Y which is the 5-digit encoding for the modulation type of the emitter PRI. $\mathcal{L}_M$ compares the squared error in the prediction of modulation type when the PRI flag of the ground truth is 1. The total loss of the proposed method can be expressed as $\mathcal{L}_{total}$ after taking the weighted sum for these three losses.

$$\mathcal{L}_{total} = \lambda^T \mathcal{L}_T + \lambda^F \mathcal{L}_F + \lambda^M \mathcal{L}_M \tag{8}$$

where λ is the weight of each task. Therefore, our MTL training can be treated as an optimization problem as follows:

$$\theta^* = \arg\min_\theta \mathcal{L}_{total}(\mathcal{D}, \theta) \tag{9}$$

where $\mathcal{D}$ is the training set for the tasks, θ is the total parameters in our MTL model.

E. WEAK LABEL MERGING

With any kind of deinterleaving method, it is almost impossible to directly estimate just the values corresponding to the PRIs of the input signal in the presence of pulse distortion. Although there is a difference depending on the degree of distortion, CWT-based methods, like other deinterleaving methods, produce multiple peaks (PRIs) in the output when a signal with pulse distortion is used for input data, making it difficult to estimate accurately. To improve the performance in the PRI estimation, we propose using weak label merging (WLM) as a post-processing step for the PRI flag vector in the network output. WLM does not directly affect training, and it operates only in the test step. WLM merges adjacent values to the largest value if there are several adjacent values estimated as the PRI of the emitter. For the modulation flag, the type with the maximum value of modulation flag for the active PRI flag in the WLM result is set as the modulation type for the PRI flag.

Algorithm 1 shows the details of WLM. It takes the two inputs, the output of network ($\hat{Y}$) and the score threshold (σ). The threshold σ determines whether merging should be performed in the corresponding PRI index. In WLM, the PRI scores of the indices adjacent to the PRI index in which the PRI score has the largest value are merged. The merging process is repeated for the next largest PRI value among the remaining PRI values. The process terminates when the largest PRI value to be merged is smaller than the threshold. Depending on the PRI modulation type in the index, which is the center of the merge, if it is stable, the merging range (τ) is set to only 1μs, as in line 9 of Algorithm 1, otherwise it is set to 3μs, as in line 11. Merging is performed on the τ range left and right from the merging basis index, as in lines 13 to 16. By merging adjacent peaks through WLM, the number of peaks generated per emitter can be reduced, and as a result, deinterleaving accuracy can be improved.

V. SIMULATIONS

A. DATA GENERATION

In this section we perform simulations to demonstrate the performance of our unified method for deinterleaving and PRI modulation recognition based on MTL with deep neural

Algorithm 1 Algorithm for WLM

Input: prediction $\hat{Y}$, score threshold σ
Output: $\hat{Y}$

$s \leftarrow$ sort $\hat{Y}$ by the descending order (index of $\hat{Y}$)
$f_i \leftarrow 0, i = 0, \ldots, n-1$
for $i = 0$ to $n-1$ **do**
  if $(\hat{Y}_{1,s_i} \leq \sigma)$ **then**
    break
  end if
  if $(f_{s_i} == 0)$ **then**
    if argmax$(\hat{Y}_{2:6,s_i}) == 0$ **then**
      $\tau \leftarrow 1$
    else
      $\tau \leftarrow 3$
    end if
    for $j = -\tau$ to τ **do**
      $\hat{Y}_{1,s_i} \leftarrow \hat{Y}_{1,s_i} + \hat{Y}_{1,s_{i+j}}$
      $\hat{Y}_{1,s_{i+j}} \leftarrow 0$
      $\hat{f}_{s_{i+j}} \leftarrow 1$
    end for
  end if
end for

networks. To analyze the performance based on a real EW environment, we applied spurious pulses and missing pulses to the input data.

Table 2 shows the parameters used to generate the input signal. Since our proposed method is based on MTL deep learning, training data and validation data are required. To train our model, we generated a total of 10,000 signals. 80% of the generated signals were used for training and the remaining 20% were used for validation to prevent over-fitting in the training step. Various PRI variation rates and pulse distortion rates were set. Each data was a pulse train consisting of a total of 512 pulses. The number of emitters in each signal of the training data were randomly chosen in the range from 1 to 4, and the modulation type of each emitter was randomly selected from the five types shown in Table 2. If the modulation type was non-stable, a range of PRI variation from 5 to 20% was randomly applied. Distortion pulses such as spurious pulse and missing pulse were applied randomly within 0∼5%. We also generated the test data with 2,000 signals for each test condition. All other parameters were set the same as in the training data, except that pulse distortion from 0% to 30% was applied in 5% increments. The SNR, which is an error factor considered in the receiver, is already reflected in the PDW, so it is not considered in this paper.

B. METRICS

In this section, we describe the metrics used for performance evaluation. Since the proposed method has two main tasks, of deinterleaving and modulation type recognition, we used separate metrics to evaluate the performance of the two tasks. In the deinterleaving task, multiple PRI values can be estimated from 100μs to 300μs. We evaluated the performance by focusing only on the positive prediction, because only a small part of the whole PRI range is activated. Finding the emitter accurately and not generating false alarms are the most important objectives in deinterleaving. Hence, we used precision P as a performance metric for deinterleaving, defined as

$$P = \frac{TP}{TP + FP} \tag{10}$$

where TP is a true positive prediction for an active emitter, and FP is a false positive prediction for a non-active emitter.

To measure PRI modulation recognition performance, we used the macro F1-score, which is one of the evaluation metrics for a multi-label classification problems [43], [44]. The F1-score includes concepts of precision and recall. First, we constructed a confusion matrix for true modulation types versus predicted modulation types using the results from PRI modulation prediction. In the output from the trained network for each input pulse train, the predicted PRI modulation types for ground-truth mean PRI value contribute to increase the count by 1 in the row of the true modulation type in the confusion matrix. For example, suppose an input pulse train has a stable (STB) modulation type with a mean PRI of 200μs, and a jittered (JTR) modulation type with a mean PRI of 275μs. If the prediction results are a stable modulation type with a mean PRI 200μs, a sliding(-) (SLM) modulation with a mean PRI 275μs, and a jittered (JTR) modulation with a mean PRI 310μs, then only the (True, Predicted) = (STB, STB) and (JTR, SLM) units in the confusion matrix are increased by 1.

For each modulation type k, precision P_k and recall R_k can be computed as follows:

$$P_k = \frac{TP_k}{TP_k + FP_k} \tag{11}$$

$$R_k = \frac{TP_k}{TP_k + FN_k} \tag{12}$$

where TP_k is a true positive prediction, FP_k is a false positive prediction, and FN_k is a false negative prediction for modulation type k. False negative prediction means that the true modulation type is not the predicted type. Fig. 13 shows an example of a confusion matrix to explain precision and recall.

TABLE 2. Parameters of the input signals.

Parameters	Value
num of pulses per signal	512
num of emitters per signal	random in [1,4]
mean PRI	100-300μs
modulations types	STB, JTR, SLP, SLM, WOB
- jitter rate (JTR)	5%-20%
- PRI variation (SLP,SLM,WOB)	5%-20%
- number of periods (SLP,SLM,WOB)	random in [3,15]
measurement error	$\pm$0.5μs
missing pulse rate	0%-30%
spurious pulse rate	0%-30%
time shift (for CWT)	32

		Predicted label				
		1(STB)	2(JTR)	3(SLP)	4(SLM)	5(WOB)
True label	1(STB)	30	0	5	4	3
	2(JTR)	3	27	5	1	2
	3(SLP)	1	0	33	2	3
	4(SLM)	3	7	3	35	6
	5(WOB)	0	1	1	4	37

FIGURE 13. An example for a confusion matrix.

$TP_1 = 30$, FP_1 correspond to the shaded block in the first column, and FN_1 is explained by the shaded block in the first row. The precision (P_1) and recall (R_1) for the STB type are calculated as follows:

$$P_1 = \frac{30}{30+3+1+3+0} \fallingdotseq 0.8108 \tag{13}$$

$$R_1 = \frac{30}{30+0+5+4+3} \fallingdotseq 0.7143 \tag{14}$$

F1-score is a harmonic mean of precision and recall, and can be calculated as follows:

$$F1_k = \frac{2 \times P_k \times R_k}{P_k + R_k} \tag{15}$$

where, $F1_k$ is F1-score for PRI modulation type k. After calculating the F1-score for each type, we can calculate the macro F1-score using their arithmetic mean as follows:

$$macro\,F1 = \frac{1}{5}\sum_{k=1}^{5} F1_k \tag{16}$$

C. RESULTS AND DISCUSSION

1) DEINTERLEAVING PERFORMANCE

We verified the performance of the proposed MTL-based deinterleaving by comparison with the conventional CWT method. The conventional CWT method estimates the PRI among peaks by comparing them with a predefined threshold. In the paper by Driscoll [13], an example was given where the threshold values were set to 0.5 and 0.6, but specific threshold values were not fixed. To derive the best performance in the conventional CWT method, we variously applied two configurable parameters, the size M of the moving window and the threshold value for PRI estimation. For four cases CWT_{16}, CWT_{32}, CWT_{64}, CWT_{80}, we used the window sizes of 16, 32, 64, 80, respectively. CWT_{pro} used the combined CWT results from two window sizes 16 and 64 as in our proposed method. For each case, the best result was chosen after applying four thresholds of 0.3, 0.5, 0.6, 0.8. For the proposed method, the score threshold(σ) for weak label merging was set to 1, and the weights of each loss function were all set equally to 1.

Fig. 14 shows the deinterleaving performance of each case, while increasing the range of change in the non-stable PRI from 5% to 20% with no pulse distortion. The conventional CWT showed big performance differences depending on the size of the moving window, and showed meaningful performance when the size of the moving window was 64 or more. It is a reasonable result that the moving window itself has a great influence on resolution when it comes to deinterleaving. It can be seen that the proposed method shows much better performance than the conventional CWT methods. While the performance of the conventional CWT methods degrades as the PRI variation rate increases, the proposed method shows stable performance regardless of the PRI change rate. For the conventional CWT method, as the range of PRI variation grows wider, the peak range appears wider. But its intensity is weaker, reducing the accuracy of the PRI estimation. On the other hand, the proposed method has already learned about the case where the range is wider and the power is weakened, so the degradation in performance is limited

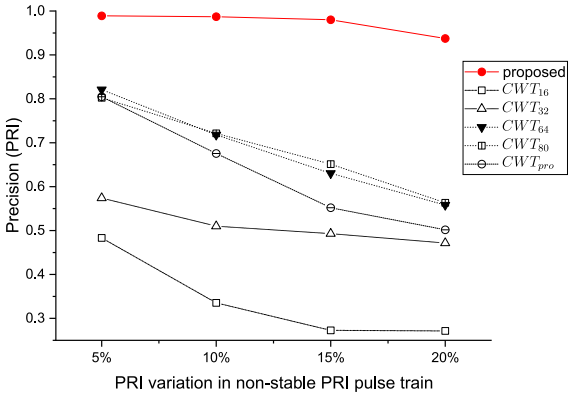

FIGURE 14. Deinterleaving precision on PRI variations (non-stable PRI).

Fig. 15 and Fig. 16 show the deinterleaving performance in a signal environment where spurious and missing pulse distortions are applied, respectively. Like the previous results, the conventional CWT method shows meaningful performance only when the size of moving window is larger than 64. The proposed method has a slightly degraded performance depending on the degree of pulse distortion, but generally

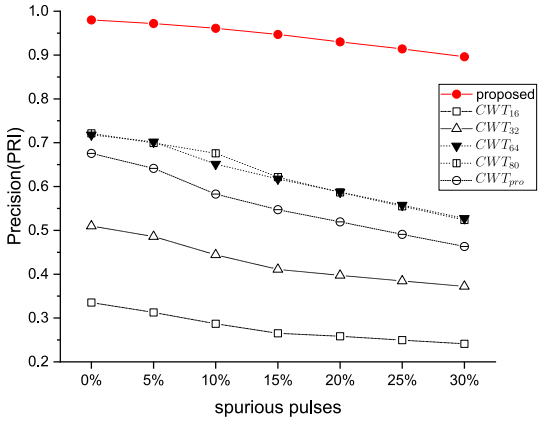

FIGURE 15. Deinterleaving precision with spurious pulses.

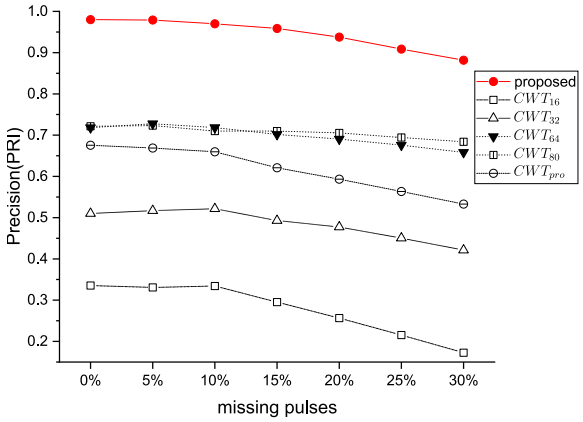

FIGURE 16. Deinterleaving precision with missing pulses.

exhibits stable performance, with a large difference in performance compared to the conventional method.

2) MODULATION RECOGNITION PERFORMANCE

Conventional modulation recognition methods analyze the modulation type of each extracted pulse train for each emitter, while our proposed method analyzes the modulation type as it is collected before each emitter is extracted. Hence, direct comparison with conventional methods is impossible. Instead, we analyzed performance under various environmental conditions as in the deinterleaving performance analysis.

To analyze the performance of the PRI modulation recognition, the estimated modulation types were compared with the ground truth. Fig. 17 shows the performance for modulation type recognition when the change rate of non-stable PRI was changed from 5% to 20%. The figure shows the F1-score for each modulation type and the macro F1-score. The interesting thing about the modulation recognition performance with PRI variations is that 10% of the change range showed better performance than the 5% change range. This is because the non-stable PRI signal only changed within 5% of the mean PRI, which created some difficulty in distinguishing it from the stable PRI. When the PRI variation range was 20%, the performance was slightly degraded, due to some overlapping with the PRI variation range of other emitters, because of the wide PRI variation range. The modulation recognition performance with PRI variation was slightly different in the non-stable PRI, but generally had a high performance, of over 99%.

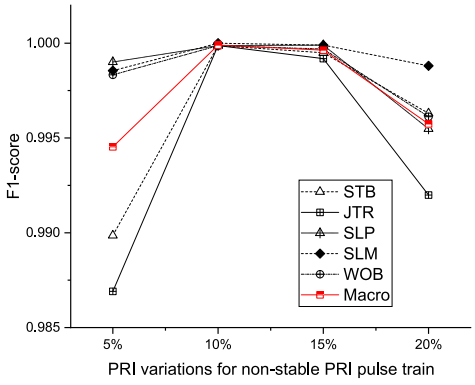

FIGURE 17. Modulation recognition performance with PRI variations (non-stable PRI).

Fig. 18 shows the PRI modulation recognition performance according to the degree of spurious pulses. The macro F1-score was used to evaluate the overall performance of the proposed model, and the F1-score for each type was used to check the performance of each modulation type. Macro F1 scores of 99% or more were obtained for up to 15% spurious pulses, but when the spurious pulse application was increased to 20%, the performance of the JTR type decreased significantly and the macro F1 score dropped to 98%. The reason the JTR type is particularly poor in performance can be understood by looking at the confusion matrix. Fig. 19 shows the confusion matrix for modulation recognition in a situation where there were 20% spurious pulses. In a situation where a lot of spurious pulses were applied, it can be seen that various types are misclassified as JTR types. In particular, since the WOB type is misclassified as JTR type with random

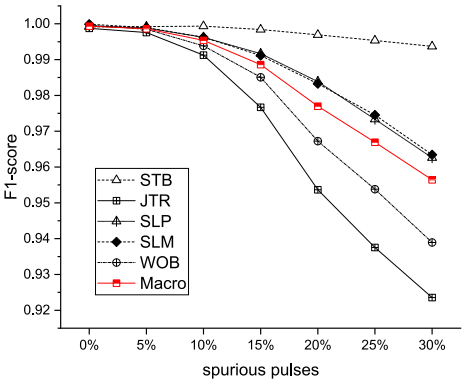

FIGURE 18. Modulation recognition performance with spurious pulses.

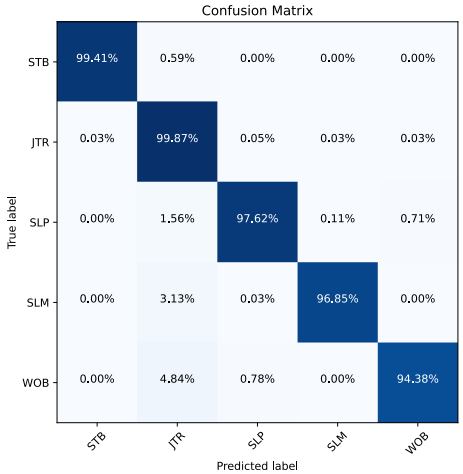

FIGURE 19. Confusion matrix with spurious pulses (20%).

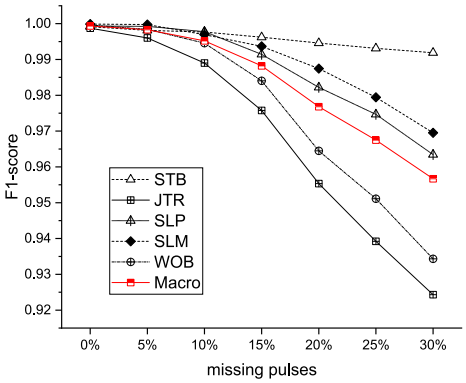

FIGURE 20. Modulation recognition performance with missing pulses.

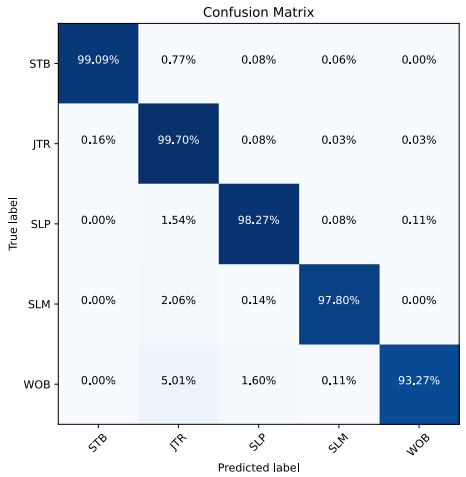

FIGURE 21. Confusion matrix with missing pulses (20%).

characteristics, it shows low performance in the F1-score of the JTR type and WOB type.

Fig. 20 shows the PRI modulation recognition performance according to the degree of missing pulses. Overall, the trend is similar to the case with spurious pulses. Although the confusion matrix in Fig. 21 is slightly different, the results are similar.

In these various simulations, our proposed method showed competent performance, even in various situations with PRI change and pulse distortions.

VI. PARAMETER SENSITIVITY

In our unified MTL-based deinterleaving and PRI modulation recognition method, the values of some parameters need to be determined for the model and label configuration. In this section, the effect of parameter values on the performance of the proposed method is shown.

A. EFFECTS OF WEAK LABEL MERGING

In this subsection, we analyze the effect of WLM on deinterleaving and modulation type recognition performance. As mentioned in Section IV-E, we determined the merging range according to the modulation type of the PRI index based on the WLM. Table. 3 shows the performance of deinterleaving according to the weak label merging parameter settings. In the table, the PRI merging range is described as (stable merging range, non-stable merging range). For example, (1,3) indicates that the merging range for stable PRI is 1μs, and the merging range for non-stable PRI is 3μs. WLM merges the scores of adjacent PRIs around the index with the largest PRI score among the surroundings. Since the encoded value of PRI modulation type does not change, the modulation recognition result is not affected. When the merging range of 3 or 4μs was set for the non-stable modulation type, stable performance was obtained regardless of the rate of PRI variation.

TABLE 3. Deinterleaving precision by WLM on PRI variations.

WLM	5%	10%	15%	20%
(0,0)	0.5499	0.5239	0.4695	0.3987
(0,1)	0.8483	0.8283	0.7892	0.6888
(0,2)	0.9470	0.9411	0.9230	0.8467
(0,3)	0.9810	0.9800	0.9712	0.9220
(0,4)	0.9841	0.9829	0.9679	0.9108
(1,0)	0.5558	0.5294	0.4770	0.4123
(1,1)	0.8542	0.8341	0.7964	0.7026
(1,2)	0.9530	0.9470	0.9301	0.8600
(1,3)	0.9873	0.9850	0.9780	0.9354
(1,4)	0.9919	0.9829	0.9691	0.9088

B. EFFECTS OF NETWORK MODEL

Our MTL model consists of a total of 12 layers, and the 2nd to 6th layers are all composed of residual blocks. We defined a total of four models as shown in Fig. 22 to verify the effect of applying the residual block. We analyzed the precision of deinterleaving task and the macro F1-score of PRI modulation recognition for each model. In order to compare performances according to models, we performed simulations under the conditions of spurious pulses and missing pulse distortions that degrade performance.

As shown in Fig. 23 to Fig. 26, the use of residual blocks is superior to that of convolution alone. Among the models where the residual block was applied, the 5_*residual* model used in our MTL model and the 6_*residual* model showed stable performance during PRI estimation and modulation recognition. As shown in Fig. 23 and 24 for the simulation results in the spurious pulses environment, the 5_*residual* model and the 6_*residual* outperformed other models. It can be seen that the overall performance of the 5_*residual* model was slightly better than that of the 6_*residual* model. The simulation results with missing pulses in Fig. 25 and 26 showed surprising performance with the residual block. In particular, Fig. 25 shows a significant performance drop in deinterleaving when the residual block was not used. When the pulse missing rate was 15∼30%, the 4_*residual* model showed some good performance, but the 5_*residual* model showed stable performance overall.

The results in this section indicate that, to ensure good performance in pulse distortion environments, it is necessary

layer no.	no_residual	4_residual	5_residual (proposed)	6_residual
1	conv	conv	conv	conv
2	conv+maxpooling	residual block	residual block	residual block
3	conv+maxpooling	residual block	residual block	residual block
4	conv+maxpooling	residual block	residual block	residual block
5	conv+maxpooling	residual block	residual block	residual block
6	conv	conv	residual block	residual block
7	conv	conv	conv	residual block
8	conv	conv	conv	conv
9	conv	conv	conv	conv
10	GAP	GAP	GAP	GAP
11	Dense	Dense	Dense	Dense
12	Reshape	Reshape	Reshape	Reshape

FIGURE 22. Model definition.

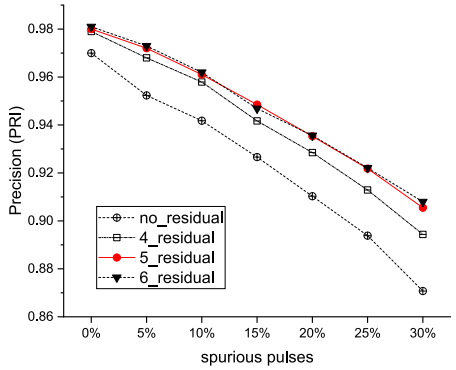

FIGURE 23. Deinterleaving precision with spurious pulses.

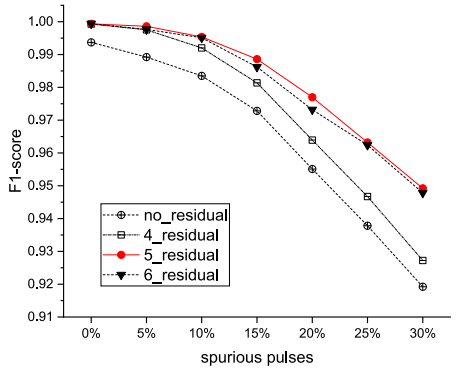

FIGURE 24. Modulation recognition performance with spurious pulses.

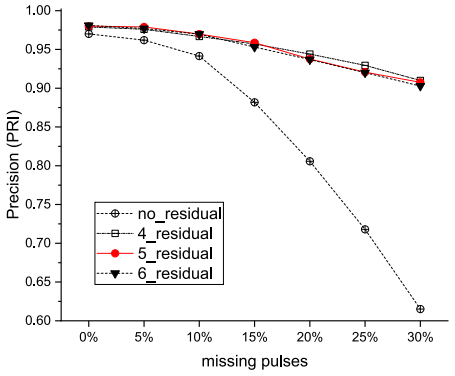

FIGURE 25. Deinterleaving precision with missing pulses.

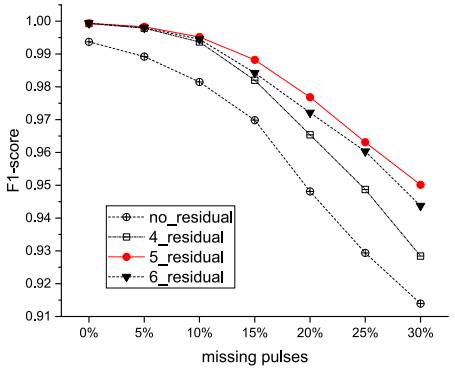

FIGURE 26. Modulation recognition performance with missing pulses.

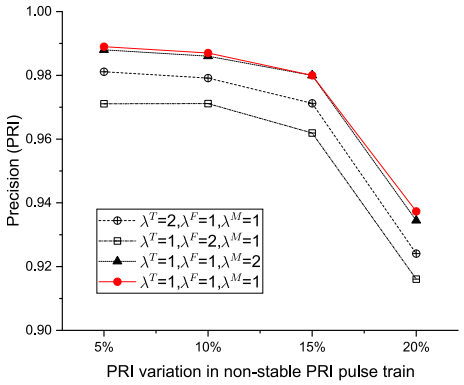

FIGURE 27. Deinterleaving precision on PRI variations (non-stable PRI).

to use an appropriate number of residual blocks. Our model applied 5_*residual*, which showed more stable performance than other residual models.

C. EFFECTS OF LOSS WEIGHTS

In Section IV-D, we defined the loss functions for three tasks, of emitter estimation, non-emitter suppression and modulation recognition, and the total loss was set as their weighted sum. In this subsection, we study the effect of the weight of each loss function on performance.

Fig. 27 to Fig. 30 show the performance of deinterleaving and PRI modulation recognition depending on the set weight applied to the loss of each task. In the figure, λ^T and λ^F represent the weight of the loss function of the emitter estimation task and the non-emitter suppression task, respectively, and λ^M represents the weight of the loss function of the PRI modulation recognition task.

The performance changed as the PRI variation in the non-stable PRI pulse train increased, as shown in Fig. 27 and Fig. 28. Giving a larger weight to either the emitter estimation task or the non-emitter suppression task had no effect on the accuracy of deinterleaving. In terms of deinterleaving, both were equally important, so giving the same weight value showed better performance. Applying a larger weight to the

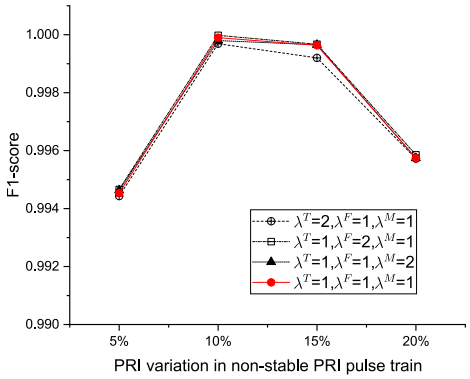

FIGURE 28. Modulation recognition performance with PRI variations.

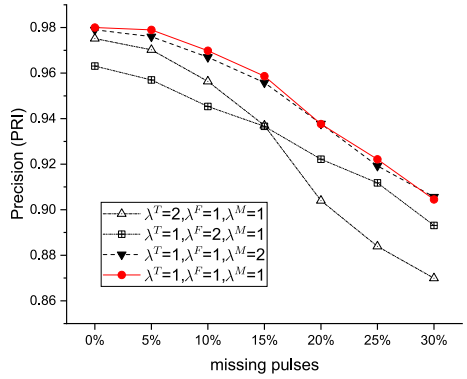

FIGURE 29. Deinterleaving precision with missing pulses.

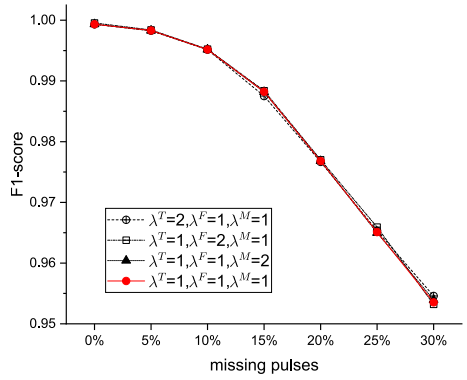

FIGURE 30. Modulation recognition performance with missing pulses.

PRI modulation recognition task made no difference to the overall performance. This is because when only modulation recognition was emphasized, the deinterleaving performance degraded.

Fig. 29 and Fig. 30 compare the performance under the missing pulses environment. Because the difference in performance was slightly bigger for missing pulses than for spurious pulses, the effect of loss weight on performance can be mainly attributed to missing pulses. PRI modulation recognition showed almost similar performance, but the best performance for deinterleaving was obtained with the same value for each loss weight.

Through several simulations, we came to the following conclusions about setting the loss weight. Focusing on finding the active emitter increased false alarms, while emphasizing suppression of the non-emitter reduced the false alarms, but reduced the accuracy of the active emitter estimation. In addition, emphasis on modulation recognition performance led to degraded deinterleaving performance. As a result, the estimated active emitter was reduced and the number of emitters for modulation recognition was reduced. Therefore, it is possible to expect stable performance under various distortion conditions by assigning the same weight to each of the two tasks, for deinterleaving and one task for modulation.

D. EFFECTS OF WINDOW SIZE

In this subsection, we analyze the effect of window size(M) on deinterleaving and PRI modulation recognition performance. Fig. 31 to Fig. 34 compare deinterleaving and PRI modulation recognition performance according to various window size settings. When the window size is small, the deinterleaving performance is degraded, but the modulation recognition performance is increased. As the window size is increased, the result is the opposite. On the other hand, when the CWT results from two window sizes are combined, high performance in both tasks was obtained.

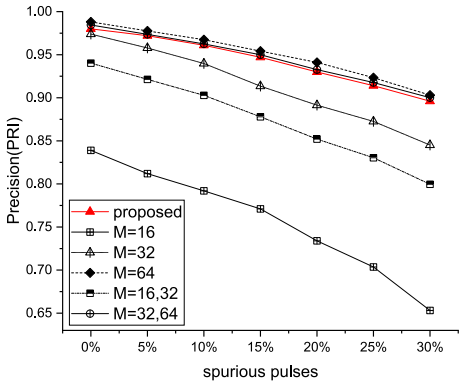

FIGURE 31. Deinterleaving precision with spurious pulses.

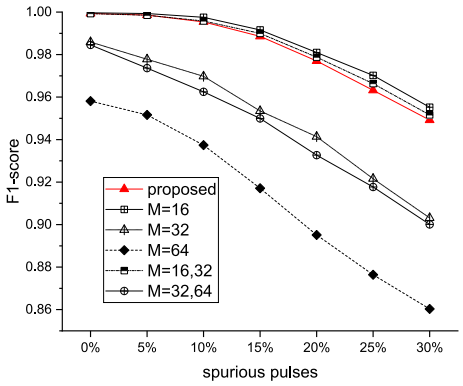

FIGURE 32. Modulation recognition performance with spurious pulses.

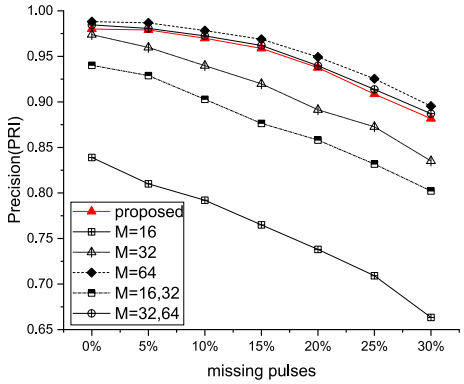

FIGURE 33. Deinterleaving precision with missing pulses.

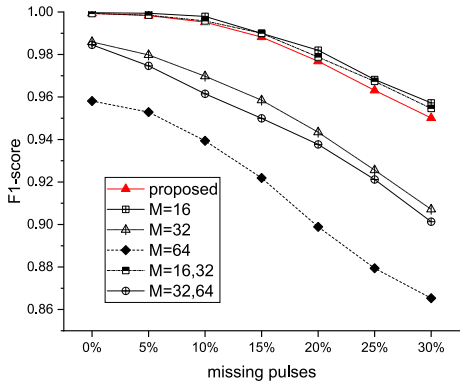

FIGURE 34. Modulation recognition performance with missing pulses.

Therefore, stable performance can be expected in both tasks by appropriately combining the results of a small M value and a large M value.

VII. CONCLUSION AND FUTURE WORKS

In this paper, we proposed a unified method based on MTL using deep neural networks to solve the two main tasks in electronic warfare - deinterleaving and PRI modulation recognition. We conducted various studies to find the model parameters suitable for our proposed MTL model, and analyzed the performance of the proposed method by comparison with the performance of the conventional CWT method in various environments, such as pulse distortions. The simulation results showed that our model estimated the PRI and modulation type of each emitter in the input pulse train with high accuracy, even with various PRI variations and in various pulse distortion environments.

For the convenience of simulation, we set the range of the PRI to be detected to 100∼300μs, but in order to operate in an actual environment, it must be able to cover the entire range of the PRI to be detected. In addition, in this paper, the research focused only on using the information between pulses, such as PRI, but it can be extended to use information in the pulse itself, such as frequency modulation or scan type analysis.

REFERENCES

[1] R. G. Wiley, *ELINT: The Interception Analysis Radar Signals*. Norwood, MA, USA: Artech House, 2006.
[2] H. Nan, S. Peng, J. Yu, and X. Wang, "Pulse interference method against PRI sorting," *J. Eng.*, vol. 2019, no. 19, pp. 5732–5735, Oct. 2019.
[3] S.-H. Kong, M. Kim, L. M. Hoang, and E. Kim, "Automatic LPI radar waveform recognition using CNN," *IEEE Access*, vol. 6, pp. 4207–4219, 2018.
[4] W. Si, C. Wan, and C. Zhang, "Towards an accurate radar waveform recognition algorithm based on dense CNN," *Multimedia Tools Appl.*, vol. 80, no. 2, pp. 1779–1792, Jan. 2021.
[5] S. Wei, Q. Qu, H. Su, M. Wang, J. Shi, and X. Hao, "Intra-pulse modulation radar signal recognition based on CLDN network," *IET Radar, Sonar Navigat.*, vol. 14, no. 6, pp. 803–810, 2020.
[6] J. Gao, Y. Lu, J. Qi, and L. Shen, "A radar signal recognition system based on non-negative matrix factorization network and improved artificial bee colony algorithm," *IEEE Access*, vol. 7, pp. 117612–117626, 2019.
[7] I. Jordanov, N. Petrov, and A. Petrozziello, "Classifiers accuracy improvement based on missing data imputation," *J. Artif. Intell. Soft Comput. Res.*, vol. 8, no. 1, pp. 31–48, Jan. 2018.
[8] H. K. Mardia, "New techniques for the deinterleaving of repetitive sequences," *IEE Proc. F, Radar Signal Process.*, vol. 136, no. 4, pp. 149–154, Aug. 1989.
[9] D. J. Milojević and B. M. Popović, "Improved algorithm for the deinterleaving of radar pulses," *IEE Proc. F, Radar Signal Process.*, vol. 139, no. 1, pp. 98–104, 1992.
[10] Y. Liu and Q. Zhang, "Improved method for deinterleaving radar signals and estimating PRI values," *IET Radar, Sonar Navigat.*, vol. 12, no. 5, pp. 506–514, May 2018.
[11] Z. Ge, X. Sun, W. Ren, W. Chen, and G. Xu, "Improved algorithm of radar pulse repetition interval deinterleaving based on pulse correlation," *IEEE Access*, vol. 7, pp. 30126–30134, 2019.
[12] R. J. Orsi, J. B. Moore, and R. E. Mahony, "Spectrum estimation of interleaved pulse trains," *IEEE Trans. Signal Process.*, vol. 47, no. 6, pp. 1646–1653, Jun. 1999.
[13] D. E. Driscoll and S. D. Howard, "The detection of radar pulse sequences by means of a continuous wavelet transform," in *Proc. IEEE Int. Conf. Acoust., Speech, Signal Process.*, vol. 3, Mar. 1999, pp. 1389–1392.
[14] K. Nishiguchi and M. Kobayashi, "Improved algorithm for estimating pulse repetition intervals," *IEEE Trans. Aerosp. Electron. Syst.*, vol. 36, no. 2, pp. 407–421, Apr. 2000.
[15] Y. Mao, J. Han, G. Guo, and X. Qing, "An improved algorithm of PRI transform," in *Proc. WRI Global Congr. Intell. Syst.*, vol. 3, 2009, pp. 145–149.
[16] Y. Xi, X. Wu, Y. Wu, and L. Deng, "A fast and real-time PRI transform algorithm for deinterleaving large PRI jitter signals," in *Proc. 37th Chin. Control Conf. (CCC)*, Jul. 2018, pp. 4465–4469.
[17] Y. Liu, Y. Chen, and S. Sun, "A radar signal sorting algorithm based on PRI," in *Proc. 19th Int. Symp. Commun. Inf. Technol. (ISCIT)*, Sep. 2019, pp. 144–149.
[18] T. Tian, J. Ni, and Y. Jiang, "Deinterleaving method of complex staggered PRI radar signals based on EDW fusion," *J. Eng.*, vol. 2019, no. 20, pp. 6818–6822, Oct. 2019.
[19] Y. Xi, X. Wu, Y. Wu, Y. Cai, and Y. Zhao, "A novel algorithm for multi-signals deinterleaving and two-dimensional imaging recognition based on short-time PRI transform," in *Proc. Chin. Autom. Congr. (CAC)*, 2019, pp. 4727–4732.
[20] B. Wang, B. Gao, L. Wang, F. Xin, and X. Song, "Radar signal sorting algorithm based on PRI for large jitter," *IOP Conf. Ser., Mater. Sci. Eng.*, vol. 466, no. 1, 2018, Art. no. 012042.
[21] F. Li, Z. Yang, and C. Yang, "Radar signal sorting technology based on image processing and Hough transform," in *Proc. Int. Conf. Microw. Millim. Wave Technol. (ICMMT)*, May 2018, pp. 1–3.
[22] Z.-M. Liu and P. S. Yu, "Classification, denoising, and deinterleaving of pulse streams with recurrent neural networks," *IEEE Trans. Aerosp. Electron. Syst.*, vol. 55, no. 4, pp. 1624–1639, Aug. 2019.
[23] X. Li, Z. Liu, and Z. Huang, "Deinterleaving of pulse streams with denoising autoencoders," *IEEE Trans. Aerosp. Electron. Syst.*, vol. 56, no. 6, pp. 4767–4778, Dec. 2020.
[24] A. Erdogan and K. George, "Deinterleaving radar pulse train using neural networks," in *Proc. IEEE Int. Conf. Comput. Sci. Eng. (CSE)*, Aug. 2019, pp. 141–147.

[25] K. Gençol, A. Kara, and N. At, "Improvements on deinterleaving of radar pulses in dynamically varying signal environments," *Digit. Signal Process.*, vol. 69, pp. 86–93, Mar. 2017.
[26] Y.-J. Ryoo, K.-H. Song, and W.-W. Kim, "Recognition of PRI modulation types of radar signals using the autocorrelation," *IEICE Trans. Commun.*, vol. E90-B, no. 5, pp. 1290–1294, May 2007.
[27] F. Katsilieris, S. Apfeld, and A. Charlish, "Correlation based classification of complex PRI modulation types," in *Proc. Sensor Signal Process. Defence Conf. (SSPD)*, 2017, pp. 1–5.
[28] G. P. Noone, "A neural approach to automatic pulse repetition interval modulation recognition," in *Proc. Inf., Decis. Control. Data Inf. Fusion Symp., Signal Process. Commun. Symp. Decis. Control Symp.*, 1999, pp. 213–218.
[29] A. Mahdavi and A. M. Pezeshk, "A robust method for PRI modulation recognition," in *Proc. IEEE 10th Int. Conf. SIGNAL Process. Proc.*, Oct. 2010, pp. 1873–1876.
[30] Y. Liu and Q. Zhang, "An improved algorithm for PRI modulation recognition," in *Proc. IEEE Int. Conf. Signal Process., Commun. Comput. (ICSPCC)*, Oct. 2017, pp. 1–5.
[31] K.-H. Song, D.-W. Lee, J.-W. Han, and B.-K. Park, "Pulse repetition interval modulation recognition using symbolization," in *Proc. Int. Conf. Digit. Image, Techn. Appl.*, 2010, pp. 540–545.
[32] Y. Tang, M. He, X. Tang, J. Han, and X. Fan, "Method for automatically identifying PRI patterns of complex radar signals," *J. Eng.*, vol. 2019, no. 20, pp. 6975–6978, 2019.
[33] U. I. Ahmed, T. ur Rehman, S. Baqar, I. Hussain, and M. Adnan, "Robust pulse repetition interval (PRI) classification scheme under complex multi emitter scenario," in *Proc. 22nd Int. Microw. Radar Conf. (MIKON)*, May 2018, pp. 597–600.
[34] K. Gençol, N. At, and A. Kara, "A wavelet-based feature set for recognizing pulse repetition interval modulation patterns," *TURKISH J. Electr. Eng. Comput. Sci.*, vol. 24, pp. 3078–3090, 2016.
[35] J.-P. Kauppi, K. Martikainen, and U. Ruotsalainen, "Hierarchical classification of dynamically varying radar pulse repetition interval modulation patterns," *Neural Netw.*, vol. 23, no. 10, pp. 1226–1237, Dec. 2010.
[36] H. P. Nguyen, H. Q. Nguyen, and D. T. Ngo, "Deep learning for pulse repetition interval classification," in *Proc. ICPRAM*, 2019, pp. 313–319.
[37] Q. Qu, S. Wei, Y. Wu, and M. Wang, "ACSE networks and autocorrelation features for PRI modulation recognition," *IEEE Commun. Lett.*, vol. 24, no. 8, pp. 1729–1733, Aug. 2020.
[38] X. Li, Z. Liu, and Z. Huang, "Attention-based radar PRI modulation recognition with recurrent neural networks," *IEEE Access*, vol. 8, pp. 57426–57436, 2020.
[39] I. Goodfellow, Y. Bengio, A. Courville, and Y. Bengio, *Deep Learn.*, vol. 1, no. 2. Cambridge, MA, USA: MIT Press, 2016.
[40] M. Lin, Q. Chen, and S. Yan, "Network in network," 2013, *arXiv:1312.4400*. [Online]. Available: https://arxiv.org/abs/1312.4400
[41] K. He, X. Zhang, S. Ren, and J. Sun, "Deep residual learning for image recognition," in *Proc. IEEE Conf. Comput. Vis. Pattern Recognit.*, Mar. 2016, pp. 770–778.
[42] Y. Zhang and Q. Yang, "A survey on multi-task learning," 2017, *arXiv:1707.08114*. [Online]. Available: https://arxiv.org/abs/1707.08114
[43] M. Grandini, E. Bagli, and G. Visani, "Metrics for multi-class classification: An overview," 2020, *arXiv:2008.05756*. [Online]. Available: http://arxiv.org/abs/2008.05756
[44] M.-L. Zhang and Z.-H. Zhou, "A review on multi-label learning algorithms," *IEEE Trans. Knowl. Data Eng.*, vol. 26, no. 8, pp. 1819–1837, Aug. 2014.

JIN-WOO HAN received the M.S. degree in computer engineering from Kyungpook National University, South Korea, in 2002. He is currently a Senior Researcher with the Agency for Defense Development, South Korea. His current research interests include radar signal processing, machine learning, and pattern recognition, especially on radar deinterleaving.

CHEONG HEE PARK received the M.S. and Ph.D. degrees in computer science from the Department of Computer Science and Engineering, University of Minnesota, in 2002 and 2004, respectively, and the Ph.D. degree in mathematics from Yonsei University, South Korea, in 1998. She is currently a Professor with the Department of Computer Science and Engineering, Chungnam National University, South Korea. Her research interests include machine learning, data mining, and pattern recognition.